Removal of basic textile dyes from water by natural and modified Algerian zeolite: kinetic, thermodynamic and equilibrium studies

Nassima Belgaid[a], *Mohamed Redha* Menani[b], *Kamel Eddine* Bouhidel[c]

[a] University of Batna 2, Laboratory of Mobilisation and Water Ressources Management (MGRE), Institute of Earth Sciences and Universe, 53, road of Constantine, Fesdis, Batna 05078, Republic of Algeria.
e-mail: n.belgaid@univ-batna2.dz, **corresponding author**,
ORCiD: https://orcid.org/0009-0008-3508-540X

[b] University of Batna 1, Laboratory of Chemistry and Environmental Chemistry (LCCE), Department of Chemistry, Faculty of Matter Sciences, road of Biskra, Batna 05000, Republic of Algeria
e-mail: redha.menani@univ-batna2.dz
ORCiD: https://orcid.org/0000-0001-7261-9417

[c] University of Batna 1, Laboratory of Chemistry and Environmental Chemistry (LCCE), Department of Chemistry, Faculty of Matter Sciences, road of Biskra, Batna 05000, Republic of Algeria
e-mail: ke.bouhidel@gmail.com
ORCiD: https://orcid.org/0009-0004-1956-7733

https://doi.org/10.5937/vojtehg73-56126

FIELD: chemical technologies
ARTICLE TYPE: original scientific paper

Abstract:

Introduction/purpose: Algerian natural zeolite (denoted NZ) was modified using hydrochloric acid (HZ) and sodium hydroxide solution (NaZ). This study investigated the impact of acid and alkaline modifications on the adsorption of two cationic textile dyes (BR_{46} and BY_{13}) from aqueous solutions.

Methods: The XRF analysis confirmed that SiO2 is the predominant mineral in all three zeolites. The XRD results revealed that NZ is primarily composed of mordenite, with chabazite and minor quartz content. The MEB-EDX analysis showed slight variations in the Si and Al content for HZ and NaZ, without significantly altering the zeolite's structure.. The effects of initial dye concentration, contact time and pH were examined in a batch system.

ACKNOWLEDGMENT: We gratefully acknowledge the textile industry (COTITEX Ain Djasser, Batna, Algeria) for kindly providing us with cationic textile dyes (BR_{46} and BY_{13}).

Results: The adsorption on NZ, NaZ and HZ increased with longer contact times, higher initial dye concentrations, and elevated temperatures. Equilibrium was rapidly attained best described using the pseudo-second-order kinetic model. Both the Langmuir and the Freundlich isotherm models fit for the adsorption data.

Conclusion: The highest dye removal efficiency was observed for NaZ, with 97.62% for BR_{46} and 98.97% for BY_{13}. The lowest removal rates occurred at pH= 8 for HZ and pH=10 for NZ and NaZ. Adsorption was spontaneous and endothermic.

Keywords: zeolite, modification, acid, alkaline, adsorption, cationic dyes

Introduction

Dyes used in paper, plastics, food, cosmetics and textile industries are among the most prevalent organic micropollutants in water. Many of these dyes are toxic and have a severe environmental impact, as they block light penetration, inhibit photosynthesis, reduce dissolved oxygen levels, hinder plant growth, enter the food chain, and bioaccumulate **(**Lellis et al, 2019**,** Aarden, 2001**)**. Additionally, many dyes are carcinogenic. Their high solubility, chemical stability, and resistance to light and heat make their removal through conventional methods challenging. Various physical and chemical techniques are used to remove dyes from industrial effluents, including coagulation **(**Li et al, 2016**)**, biological treatments **(**Aravindhan et al, 2023**),** flotation, oxidation, and adsorption. Among these, adsorption is the most widely used due to its high efficiency, low material cost, simple design and operation, and the abundance and non-toxicity of materials like: activated carbon **(**Kumar et al, 2023**)**, silica gel, bentonite **(**Selim et al, 2014**),** kaolinite **(**Ighnih et al, 2023**)**, and zeolite **(**Senguttuvan et al, 2022**) .**

Zeolites are microporous hydrated aluminosilicates with a three-dimensional framework that carries a negative charge balanced by exchangeable cations, primarily Na^+, Ca^{2+} and K^+**.** Naturally occuring in zeolitic-rich rocks, zeolites exist in various forms, including clinoptilolite, heulandite, faujasite, mordenite, chabazite, analcime, etc. They can also be synthesized in laboratories into other forms such as zeolite A, zeolite Y, and zeolite P **(**Reeve and Fallowfield, 2018**)**. Although synthetic zeolites are valued for their high purity, large surface area, and considerable porosity, their production requires expensive raw marterials, complex synthesis processes, and time-consuming steps. Consequently, recent research has focused on enhancing the properties of natural zeolites such as exchange capacity, and a specific surface area through

various modificaton methods, including acid activation (Pastukhov et al, 2023), alkaline activation (Ates and Akgül, 2016), iron oxide modification and organic modification (Wang et al, 2023), and surfactant modification (Ebsa, 2023). The effectiveness of modifications depends not only on the target pollutant but also on the desired properties, environmental impact (toxicity), and cost considerations (expenses and duration). Therefore, a comprehensive understanding of the caracteristics, structure, morphology, and interractions of zeolites is essential, providing valuable insights for future studies.

Zeolites have a broad range of applications, from agriculture and wastewater treatment to petroleum refining, where they serve as adsorbents, molecular sieves, and ion–exchange agents (Visa, 2016).

Mordenite, first discovered in 1864 in Nova Scotia, Canada, and named after the small community of Morden, is a zeolite mineral with the molecular formula (Na^{+}_{8}) $[(AlO_2)_8(SiO_2)_{40}].24H_2O$. The Si/Al ratio in natural mordenite samples varries from 4 to 6, with higher ratios correlating to greater thermal and chemical stability (Nakamoto et al, 2017, Mamo et al, 2015). In Algeria, mordenite-type zeolite is particulary predominant in the northeast region (Mehdi et al, 2022). While its primary application has been in cement activities, only a few studies have explored its potential for removing heavy metals (Mehdi et al, 2022) and dyes (Imessaoudene et al, 2024) from water. The modification of natural zeolites using acid and alkaline solutions significantly impact their composition, morphology and porosity. These treatments facilitate the removal of silicon and aluminum from the zeolite framework, altering the SiO_2/Al_2O_3 ratio and influencing their adsorption properties, leading to the modification of external and internal surface properties (Garcia-Basabe et al, 2010).

In this work, our main objective is to improve properties of natural mordenite such as exchange capacity, specific surface and porosity via treatment with HCl and NaOH solutions without altering the main structure. This is verified by studying the adsorption capacity of two cationic textile dyes by natural and modified mordenite. The effects of contact time, initial dye concentration, pH, and temperature were aslo studied.

Materials and methods

Natural zeolite was obtained from a Tuf deposit in Tinedbar, located in Bejaia, northeast of Algeria. The bulk sample was crushed into smaller particles of varying sizes and subsequently sieved using a column sieve to obtain clay particles with a diameter of<63µm. The processed zeolite

was stored in a polyethylene container for further use and designated as NZ.

The following chemicals were used in the study: sodium hydroxide (NaOH,40g/mol, 99%), sulphuric acid (H_2SO_4, 98.08g/mol, 95-97%, d=1.83), hydrochloride acid (HCl,36.5g/mol, 37%, d= 1.18), sodium chloride (NaCl, 58.44 g/mol, 99.5%), and nitric acid (HNO_3, 63.01 g/mol, 69%, d=1.410). All reagents were obtained from Sigma-Aldrish, VWR Prolabo Chemicals, and Fluka Chemicals. Distilled water was used to prepare all solutions.

The textile dye Basic Red 56 (BR_{56} , $C_{18}H_{21}BrN_6$, 401.3 $g.mol^{-1}$) and Basic Yellow 13 (BY_{13}, $C_{20}H_{23}ClN_2O$, 342.86 $g.mol^{-1}$, pK_a =10.35) (Figure 1) were supplied from a textile industry plant located in Ain Djasser, Batna, in the eastern region of Algeria. Both dyes are cationic, water-soluble, and commonly used for dyeing acrylic fibers and textile printing.

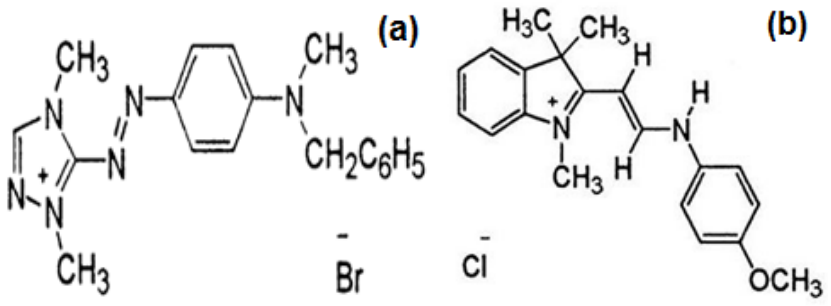

Figure1 – Structure of cationic dyes:(a) Red dye (BR56), and (b)Yellow dye (BY13)

Preparation of adsorbents

A bulk sample of natural zeolite was ground into small particles using an industrial crusher. The crushed material was then passed through a series of sieves with diameters ranging from 1 mm to 63 μm (from 15 to 236 mesh). Zeolite particles with a diameter of <73 μm were collected, stored in bottles, and designated as NZ.

Alkaline modification:

The activation of natural zeolite using an alkaline treatment was conducted as follows:

A measured mass of natural zeolite was mixed with a specific volume of sodium hydroxide solution (500 mol/m^3) at a 2:1 volume-to-mass ratio. The mixture was stirred continuously for six hours while maintaining a

temperature of 343 K. The resulting slurry was then washed several times with deionized water, filtred, dried, and sieved to 63 µm before being stored in bottles and labeled as NaZ.

Acid Activation:

The acid activation of zeolite was carried out using the following procedure:

A 5×10^{-4} m^3 reactor equipped with a reflux condenser, a magnetic stirrer, and a thermometer was used. A specified amount of natural zeolite was mixed with a hydrocloridric acid solution (500 mol/m^3) and added to the reactor. The mixture was heated under reflux at 90 °C and agitated for two hours, maintaining a constant temperature throughout the process. The clay was then filtered and repeatedly washed with deionized water until no residual acid was detected (i.e., no white precipitate appeared after the addition of barium chloride). The clay was dried at 110 °C, crushed, sieved to 63 µm, and stored in a bottle, labeled as HZ.

Results and discussion

Characterisation of adsorbents

The chemical composion of the samples was determined using X ray fluorescence (XRF). The X-ray diffraction patterns were rfomed on a diffractometer (Rigaku Miniflex II desktopX-ray diffractometer) with Cu(K_α) radiation, operated at a voltage of 40 kV and a current of 40 mA. The samples were scanned over a 2θ range from 2° to 60° at a scanning rate of 5 deg/min.The morphology of both natural and modified zeolites was analyzed using a scanning electron microscope (SEM, JEOL, JSM-6400). Additionally, FTIR spectra were recorded within the wavenumber range of 500-4000 cm^{-1} using a JASCO spectrophotometer.

Point of zero charge (PZC)

The point of zero charge (PZC) for the three zeolites (NZ, NaZ, and HZ) was determined by mixing a series of 5×10^{-5} m^3 NaCl solutions (5 mol/m^3) with the initial pH values ranging from 3 to 10 by adding 100 mol/m^3 of HNO_3 or NaOH before adding 0.05 g of zeolite. The mixture was stired for 48 hours, after which the final pH was measured. The pH variation ($\Delta pH= pH_f-pH_i$) was plotted against the initial pH.

The PCZ was identified as the intersection point of the curve where $\Delta pH=0$**.** According to the plot shown in Figure 2, the PZC values for NZ, NaZ, and HZ were determined to be 9.292, 9.71 and 7.25, respectively.

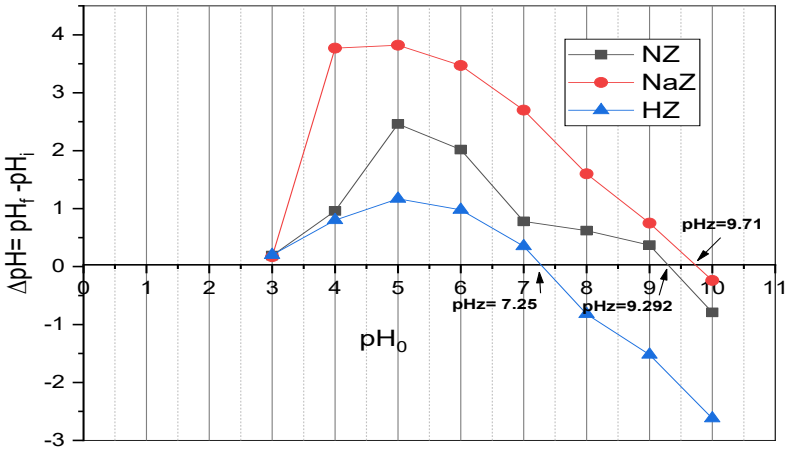

Figure 2 – Zero point of charge value for natural (NZ) and activated zeolites (NaZ and HZ)

X-ray fluoerescence (XRF)

Table 1 shows that SiO_2 is the predominant mineral in all zeolites, followed by Al_2O_3, Fe_2O_3, CaO, K_2O, and other oxides. The Si/Al ratio of NZ indicates that it belongs to the mordenite type (3 < Si/Al < 5). For the two modified zeolites (NaZ and HZ), a slight change in the ratio is observed, although the mordenite structure remains unchanged. The decrease in the silica content for NaZ is attributed to its removal by sodium hydroxide, whereas the decrease in the aluminum content for HZ is due to its removal by hydrochloric acid.

Table 1 – Chemical composition of natural zeolite (NZ), modified zeolites with 100 mol/m^3 of NaOH (NaZ) and 100 mol/m^3 of HCl (HZ)

	SiO_2	Al_2O_3	Fe_2O_3	CaO	MgO	Na_2O	K_2O	Cl	SO_3
NZ	60.43	16.01	6.57	4.42	0.88	2.41	3.55	0.015	0.025
NaZ	55.94	17.31	6.11	2.96	0.66	6.78	6.38	/	/
HZ	58.17	13.62	6.03	5.58	0.79	2.31	3.05	/	/

X-ray diffraction (XRD)

The X-ray spectra of natural zeolite and treated zeolites (NaZ and HZ) (Figure 3) indicate that mordenite is the major component of NZ, followed by chabazite and minor amounts of quartz.

A comparison of the three diffractograms reveals a shift in the peaks and a reduction in the intensity of some peaks corresponding to impurities. Additionally, an increase in the intensity of the peaks related to mordenite and chabazite was observed, demonstrating the effectiveness of acid and alkali treatments.

Furthermore, a decrease in the intensity of quartz peaks was observed for NaZ, which is attributed to the removal of Si from the framework by acid. Based on the previous studies, NZ mainly contains mordenite ($(Ca, Na_2, K_2)Al_2Si_{10}O_{24}\cdot 7H_2O$), chabazite ($Ca_2Al_2Si_4O_{12}.\ 6H_2O$), and quartz ($SiO_2$).

The reduction in the HZ peak intensities was mainly caused by the decrease in crystalinity and/or the crystal size of the mordenite framework. This explains why the mordenite structure remained intact and protected after the treatment process.

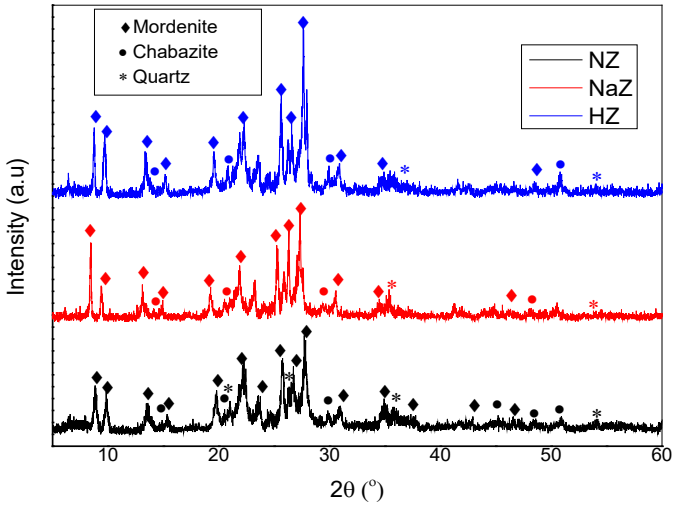

Figure 3 – XRD patterns for NZ,NaZ and HZ

Scanning electron microscopy (SEM/EDX)

The SEM images are presented in Figures 4a, 4c, and 4e. Figure 4c reveals that NaZ exhibits a slightly rougher surface and particle irregularity, mainly due to severe crystal de-agglomeration of the zeolite. In contrast, Figure 4e of HZ particles shows the presence of ultrafine/nanoscale entities surrounding larger particles.

The EDX results presented in Figure 4b, 4d, and 4f indicate changes in the chemical composition of NaZ and HZ compared to that of NZ. A slight decrease in Si and Al percentage and an increase in Na and Ca

percentage are observed for NaZ and HZ. Additionally, a significant decrease in the K content was noted in NaZ compared to NZ and HZ, probably due to ion exchange of K ions with Na ions.

The Si/Al ratio in HZ increases due to aluminum removal, while it decreases for NaZ due to the removal of Si. The oxygen content in all three zeolites is higher, probably because either all cations are present in their oxide form or part of the oxygen comes from water molecules and hydronium ions adsorbed on the surface. These findings are consistent with previous results reported by Lycourghiotis et al.(Lycourghiotis et al, 2018).

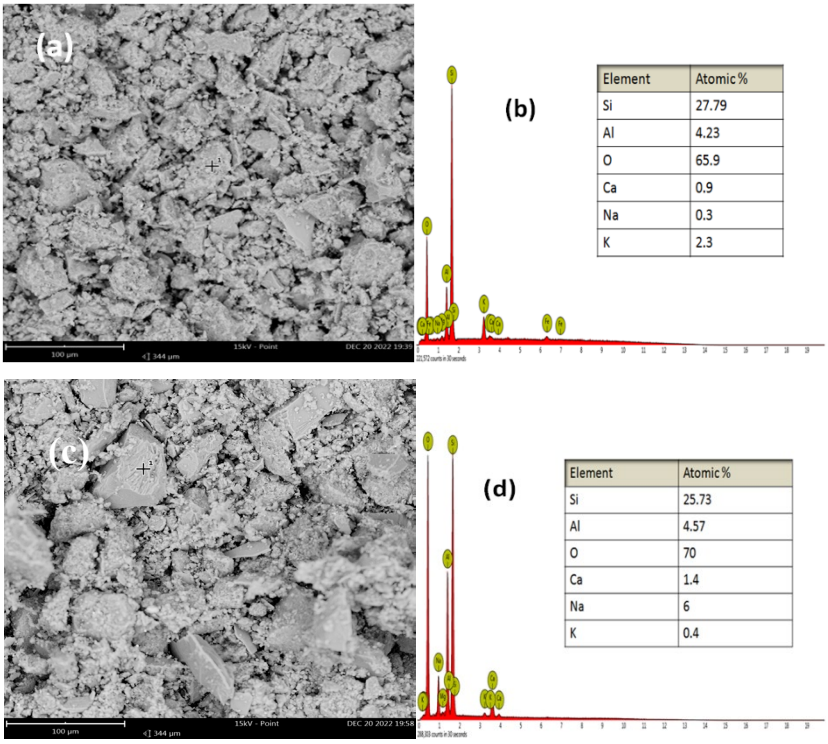

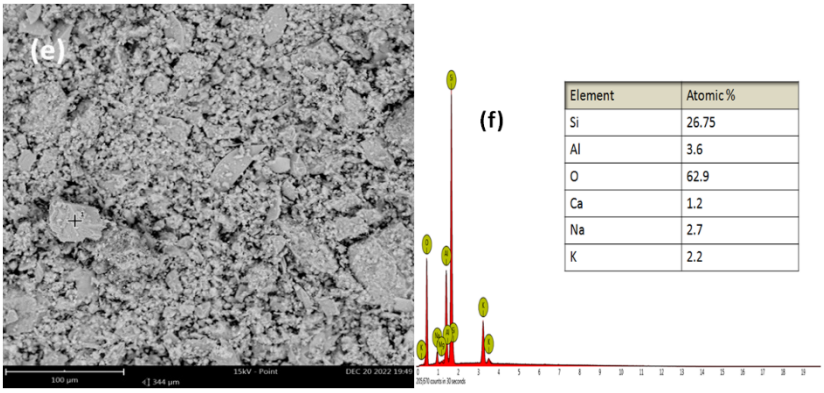

Figure 4 – SEM images and the EDX spectra of NZ (a.b), NaZ (c,d) and HZ (e,f)

Fourrier transform infra red spectroscopy (FTIR)

FTIR spectras are used to detect functional groups. Figure 5 presents the IR spectra of NZ, NaZ, and HZ. For natural zeolite (NZ), the absorption bands at 3639-3442 cm^{-1} correspond to the stretching vibrations of isolated silanol groups (Si-O-H) and H_2O molecules adsorbed on the surface. The band at 710 cm^{-1} is characteristic of the tetrahedral units of SiO_4 and AlO_4.

During the acid treatment, a shift in the main peak from 1075 cm^{-1} to 1032 cm^{-1} was observed, which can be explained by the removal of cations (mainly sodium) from the pores, affecting the vibration frequencies. At 1745 cm^{-1}, an increase in the peak intensity indicates a higher concentration of H_2O/H_3O^+ replacing cations within the framework pores, leading to an increase in microporosity and smaller mesopore volume.

Additionally, the increase in the peak size at 3607 cm^{-1} was caused by the replacement of cations by water molecules and hydronium ions (H_3O^+) on the outer surface.

For the zeolite treated with sodium hydroxide, the intensity of the peak signal at 1543 cm^{-1}, which corresponds to Al sites on the zeolite surface, shows an increase of intensity due to the removal of Si. Additionally, the intensity of the peaks in the range of 600-800 cm^{-1}, associated with exchangeable cations, decreases due to the loss of cations and silica.

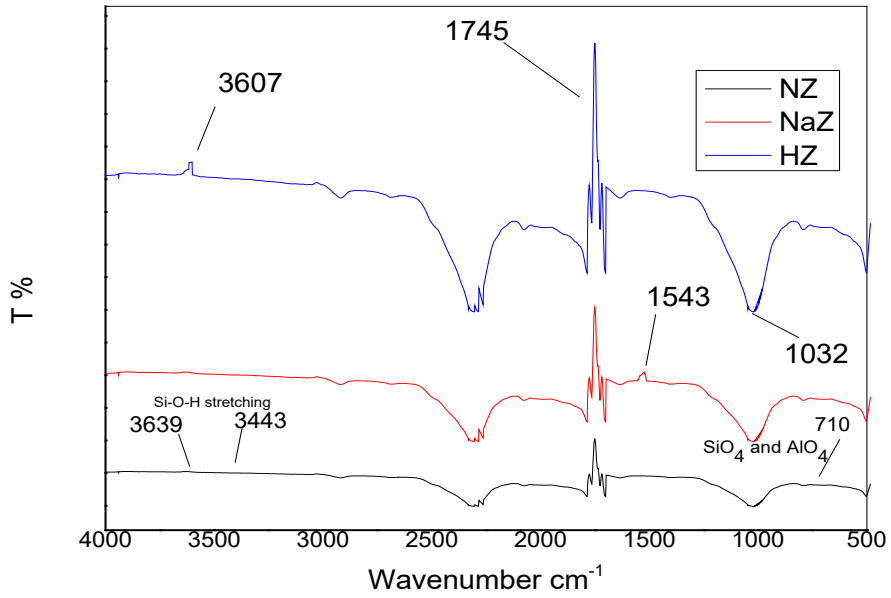

Figure 5 – FTIR spcetra of natural and modified zeolites

Adsorption isotherms modeling

The adsorption experiments were conducted in 100 cm^3 Erlenmeyer flasks by mixing 4 g/l of the adsorbent with 50 cm^3 of an aqueous dye solution. The mixture was agitated at 250 rpm for a specified period, followed by centrifugation at 2000 rpm for 10min.

The dye absorbance was measured using a SHIMADZU UV-Visible spectrophotmeter at the maximum wavelength specific to each dye: 411 nm for BY_{13}, and 532 nm for BR_{56}. The percentage of dye removal was calculated using the following equation :

$$R\% = \frac{(C_0 - C_e)}{C_0} \times 100 \quad (1)$$

The amount of adsorbed dye was calculated as follows:

$$q_e = \frac{(C_0 - C_e) \times V}{m} \quad (2)$$

where C_0 and C_e represent the initial and equilibrium concentrations of the dye in the solution (mg/l). V is the volume of the solution (L), and m is the mass of the adsorbent (g).

The equilibrium adsorption of BR_{56} and BY_{13} onto NZ, NaZ and HZ was analyzed using the Langmuir and Freundlich isotherm models. These adsorption isotherms reflect the relationship between the amount of dye adsorbed onto adsorbents (q_{ads}) and the dye concentration at equilibrium (C_e).

Langmuir isotherm

The Langmuir isotherm describes a simple model for monolayer adsorption on surfaces with identical adsorption sites. The general equation is as follows:

$$q_e = \frac{1 + K_L \cdot C_e}{1 + a_L \cdot C_e} \quad (3)$$

After linearization, Equation (3) becomes:

$$\frac{C_e}{q_e} = \frac{1}{K_L} + \frac{a_L \cdot C_e}{K_L} \quad (4)$$

where K_L and a_L are the equilibrium constants, q_e and C_e are the adsorption capacity and the concentration at equilibrium, respectively. The lineair Langmuir plot is obtained by plotting C_e/q_e versus C_e.

Freundlish isotherm

The Freundlish isotherm describes non-ideal and multilayer adsorption on a heterogenous surface. The model is given as follows:

$$q_e = K_F \cdot C_e^{\frac{1}{n}} \quad (5)$$

The linear form of Equation (5) for data fitting is expressed as follows:

$$\log q_e = \log K_F + \frac{1}{n} \log C_e \quad (6)$$

where K_F and n are the Freundlish constants, representing adsorption capacity and intensity, respectively.

Modelisation of adsorption kinetics

For a better analysis of the adsorption process, the kinetic data reported here have been fitted to three commonly kinetic models: the pseudo-first–order model, the pseudo-second-order **(**Lagergren, 1898**)**, and **(**Ho and Mckay, 1998**)**, and the intra-particule diffusion model **(**Weber Jr and Morris, 1964**)**.

The pseudo-first-order equation can be expressed as follows:

$$\frac{dq_t}{dt} = K_1 \cdot (q_e - q_t) \quad (7)$$

where K_1 is the adsorption constant rate (s^{-1}), q_t is the amount of adsorbed adsorbate at the time t ($\mu g.g^{-1}$), and q_e is the amount adsorbed at saturation. The integrated form of Equation (7) becomes (8):

$$\log(q_e - q_t) = \log q_e - K_1 \cdot t \quad (8)$$

The pseudo-second-order equation can be expressed as follows:

$$\frac{dqt}{dt} = K_2 (q_e - q_t)^2 \quad (9)$$

where K_2 is the adsorption constant rate. The integrated form of Equation (9) becomes (10):

$$\frac{t}{q_t} = \frac{1}{K_2} q_e^2 + \frac{t}{q_e} \quad (10)$$

Several factors can limit the adsorption kinetics, including intra-particle diffusion. The influence of this latter can be interpreted by the following equation:

$$q_t = K_{id} \cdot t^{\frac{1}{2}} + C \quad (11)$$

where K_{id} is the intra-particle diffusion rate constant ($\mu g.\ g^{-1}\ min^{½}$), and C is a constant related to the thickness of the boundary layer.

Thermodynamic study

The thermodynamic parameters ΔG, ΔH and ΔS can be calculated by the following equations:

$$K_c = \frac{q_e}{C_e} \quad (12)$$

$$\Delta G = -RT \ln K_c \quad (13)$$

$$\Delta G = \Delta H - T\Delta S \quad (14)$$

$$\ln K_c = \frac{\Delta S}{R} - \frac{\Delta H}{RT} \quad (15)$$

where K_c is the equilibrium constant, q_e the amount of dye adsorbed per liter of the solution at equilibrium (mg/dm^3), C_e is the equilibrium concentration of the adsorbate in the solution (mg/dm^3), T is the temperature (K), and R is the gas constant and is equal to 8.314 J/(mol K). ΔG, ΔH, and ΔS are standard free energy, standard enthalpy and standard entropy, respectively. ΔH and ΔS are caculated from the slope and the intercept of the linear plot of 1/T versus LnK_C.

Results and discussion

Adsorption study of BR_{56} and BY_{13} on natural and activated zeolites

Kinetic study

The effect of contact time on dyes removal by the zeolites (Figure 6) was studied over a range of contact times from 10 to 360min at 298 K. The initial dye concentration was set at 50mg/l, with an adsorbent dosage of 4 kg/m^3.

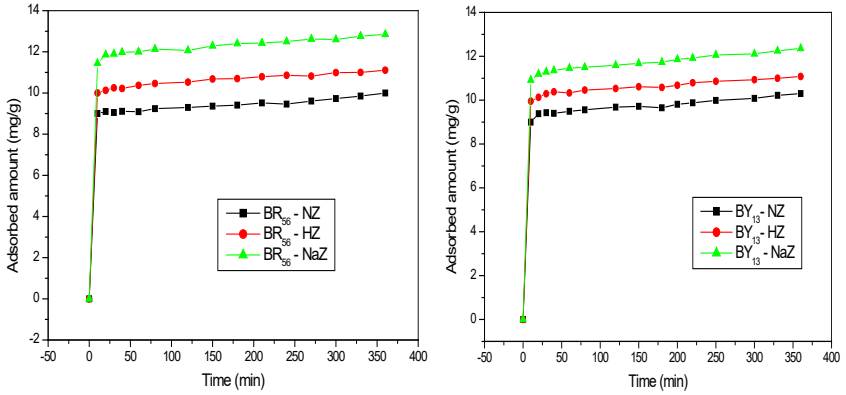

Figure 6 – Effect of the contact time on the adsorption of BR_{46} and BY_{13} on NZ, HZ and NaZ

Figure 6 illustrates that the amount of dye adsorbed increased rapidly during the first 10 min before gradually stabilizing until equilibrium was reached. The optimal time to attain equilibrium was determined to be 60 minutes. The high adsorption efficiency can be attributed to the availability of abundant active sites on the adsorbent surface. This initial rapid uptake is followed by a slower removal rate as the adsorbent reaches a saturation point. It is noteworthy that the highest adsorption capacity was observed for NaZ with both dyes, followed by HZ, whereas NZ exibited the lowest

adsorption capacity. This suggests that modifying mordenite with both acid and base enhances adsorption capacity by removing cations from the framework channels, thereby creating mesopres and micropores and increasing the overall porosity of zeolite. Lycourghiotis et al. (Lycourghiotis et al, 2018) also demonstrated that acid modification improves the porosity and structure of mordenite. However, in contrast to their study, which employed high-concentration acid, our study utilized low-concentration acid, resulting in only a slight removal of cations without significantly altering the main structure. For alkaline modification, the removal of Si and the incorporation of Na led to an increase in the number of strong acid sites, thereby enhancing the adsorption potential.

The pseudo-second-order model was applied to evaluate the adsorption of cationic dyes onto NZ, NaZ and HZ, as depicted in Figure 7. The pseudo-second-order constants are summarized in Table.2.

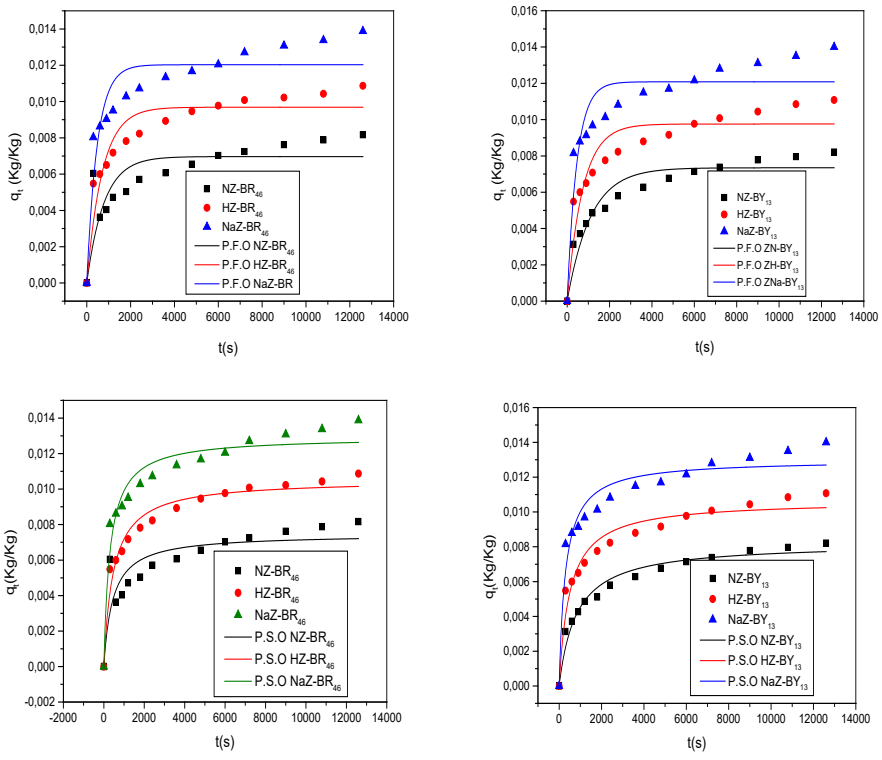

Figure7 – Application of the pseudo-first and –second-order models on the adsorption of BY_{13} and BR_{46} on NZ,NaZ, and HZ

Table 2 – Pseudo-order constants

		Pseudo First Order		
	R^2	χ^2	q_e	K_1
		BR_{46}		
NZ	0.519	1.808×10^{-6}	0.0069	0.0012
NaZ	0.588	9.124×10^{-7}	0.0096	0.0014
HZ	0.658	1.717×10^{-6}	0.012	0.0021
		BY_{13}		
NZ	0.605	4.73×10^{-7}	0.0073	9*10-4
NaZ	0.670	1.103×10^{-6}	0.007	0.0013
HZ	0.754	1.792×10^{-6}	0.012	0.00217
		Pseudo Second Order		
	R^2	χ^2	q_e	K_2
		BR_{46}		
NZ	0.941	1.204×10^{-6}	0.0074	0.304
NaZ	0.962	3.09×10^{-7}	0.010	0.204
HZ	0.944	6.77×10^{-7}	0.0129	0.252
		BY_{13}		
NZ	0.968	1.639×10^{-7}	0.0082	0.149
NaZ	0.950	4.21×10^{-7}	0.010	0.189
HZ	0.941	7.16×10^{-7}	0.013	0.258

The kinetic data presented in the table compare the pseudo-first-order and pseudo-second-order models in describing the adsorption process. The parameters analyzed include the coefficient of determination (R^2), the chi-square error (χ^2), the equilibrium adsorption capacity (q_e), and the rate constant (K).

The accuracy of the kinetic models is primarily assessed using R^2 and χ^2. The pseudo-first-order model exhibited relatively low R^2 values, ranging from 0.292 to 0.776, indicating a week to moderate correlation between the experimental and theoretical data. Additionally, the higher χ^2 values suggest significant deviations between the predicted and experimental adsorption capacities. Conversely, the pseudo-second-order model demonstrated substantially higher R^2 values (0.951-0.968), indicating a superior fit. The corresponding lower χ^2 values confirm a reduced error between theoretical and experimental data, further supporting the suitability of this model.

The equilibrium adsorption capacity (q_e) predicted by the pseudo-second-order model is more consistent with the experimental values compared to the pseudo-first-order model. This stability suggests that the pseudo-second-order model more accurately describes the adsorption process. Furthermore, the rate constant (K) values obtained from this model are lower, which may indicate a slower but more controlled adsorption mechanism. This trend aligns with the previous studies where the pseudo-second-order kinetics have been associated with chemisorption-dominated processes (Amin et al, 2023).

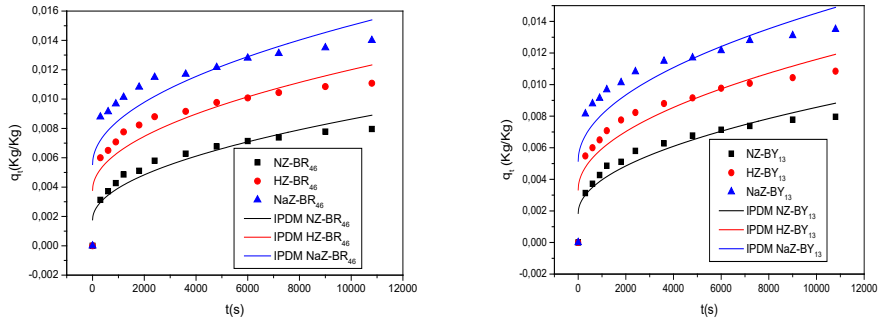

Figure 8 – Application of the intra-particule diffusion model to dye adsorption on NZ, NaZ and HZ

Table 3 – Constants of intra-particle diffusion

Constants of intra-particle diffusion	R^2	$K_{id}\times10^{-5}$ (kg/kg s)	$C_{id}\times10^{-3}$ (kg/kg)
NZ-BR_{46}	0.892	6.865	1.7
HZ-BR_{46}	0.771	8.22	3.78
NaZ-BR_{46}	0.681	9.483	5.5
NZ-BY_{13}	0.893	6.714	1.8
HZ-BY_{13}	0.813	8.564	3.3
NaZ-BY_{13}	0.709	9.375	5.15

The results indicate that adsorption does not follow to a single linear diffusion model, suggesting the presence of multiple rate-limiting steps. This non-linearity necessitates a more in-depth analysis of the diffusion rate constant (K_{id}), the boundary layer effect (C_{id}), and the correlation coefficient (R^2). The non-zero values of C_{id} (ranging from 2 to 5.465)

confirm that adsorption is influenced by boundary layer resistance, implying that film diffusion also plays a significant role in the overall process. The increase in C_{id} values with zeolite modification suggests that surface interactions contribute substantially to adsorption kinetics. The highest C_{id} values, observed for NaZ-BR_{46} (5.5) and NaZ-BY_{13} (5.15), indicate that surface adsorption effects are more pronounced in these materials, further supporting the hypothesis of multi-stage adsorption.

The variation in R^2 values (0.681-0.893) reflects differences in the extent to which intraparticle diffusion governs the adsorption process across different zeolite modifications. The highest R^2 values observed for NZ-BR_{46} (0.829) and NZ-BY_{13} (0.893), suggest a stronger correlation with the intraparticle diffusion model, whereas the lower values for NaZ-BY_{13} (0.703), indicate a more complex adsorption mechanism involving multiple kinetic stages.

Natural zeolite exhibited the lowest K_{id} values (0.485-0.487 mg/g $min^{0.5}$), presumably due to increased pore accessibility and surface acidity, which enhance adsorbates-adsorbent interactions.

The non-linearity observed in the diffusion plots suggests the presence of distinct adsorption phases:

I. External Mass Transfer Phase: Initially, dye molecules migrate from the bulk solution to the zeolite surface. The significant C_{id} values suggest that this phase is not negligible and that film diffusion contributes to the overall rate limitation.
II. Intraparticle Diffusion Phase: Once adsorbates reach the surface, they diffuse into the internal structure of zeolite. The variation in K_{id} values among different zeolites confirms that this phase is influenced by structural and chemical modifications.
III. Equilibrium Phase: At longer contact times, the adsorption rate decreases as active sites become occupied. The lower slopes observed in the latter stages of adsorption support this trend, consistent with diffusion-limited kinetics.

Effect of dye concentration

The effect of dye concentration on the adsorption on natural and activated zeolites (Figure 9) was investigated by varying the initial dye concentration between 10 and 200ppm.

The findings demonstrate that an increase in the initial dye concentration enhances dye removal efficiency. As the concentration increased from 10 to 200 ppm, both the removal percentage and the amount of dye adsorbed exhibited the following trends:

- NZ-BR_{46} : The removal efficiency increased from 44.8% to 70.84% corresponding to an increase in adsorption capacity from 1.1 to 35.5 mg/g.
- NZ-BY_{13} : The removal efficiency increased from 46.7% to 69.25% corresponding to an increase in adsorption capacity from 1.54-34.5 mg/g).
- HZ-BR_{46}: The removal efficiency increased from 55.3% to 76.88% corresponding to an increase in adsorption capacity from 1.38-38.40mg/g.
- HZ-BY_{13}: The removal efficiency increased from 56.7% to 80.43% corresponding to an increase in adsorption capacity from 1.417-40.5mg/g.
- NaZ-BR_{46}: The removal efficiency increased from 85.16% to 97.62% corresponding to an increase in adsorption capacity from 2.12-48.35mg/g.
- NaZ-BY_{13}: The removal efficiency increased from 87% to 98.97% corresponding to an increase in adsorption capacity from 2.175-49.45mg/g.

These findings suggest that dye adsorption is direcly dependent on the initial dye concentration in the solution. The observed variations in the adsorption efficiency among different zeolites highlight the influence of surface properties and activation methods on the adsorption process.

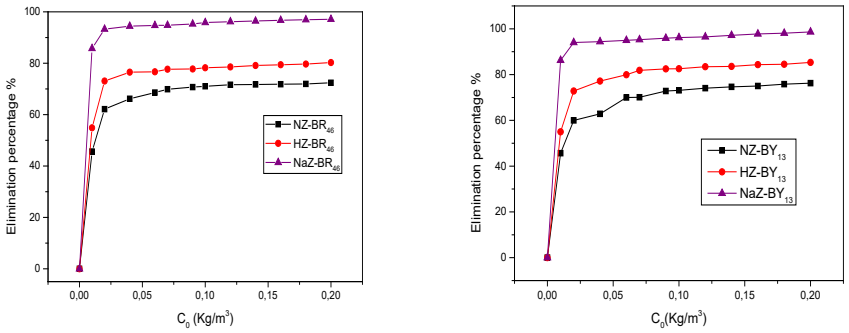

Figure 9 – Effect of the initial concentration on the adsorption of dyes on natural and activated zeolites

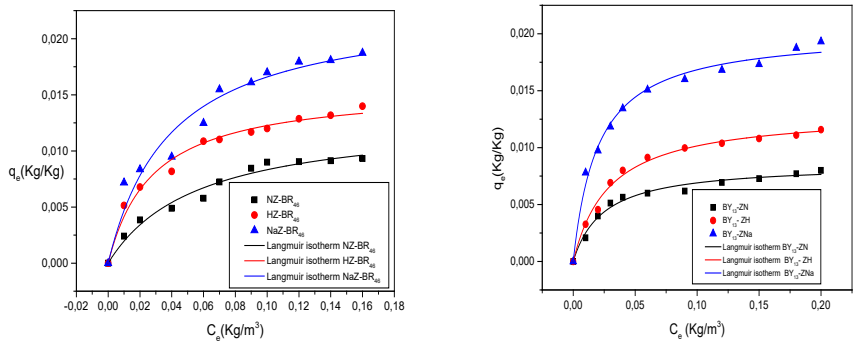

Figure 10 – The non-linear Langmuir adsorption isotherms for BR_{46} (on the left) and BY_{13} (on the right) adsorption on NZ, NaZ, and HZ

Table 4 – Langmuir constants for the adsorption of BR_{46} and BY_{13} on NZ, NaZ, and HZ

	Langmuir isotherm			
	R^2	$\chi^2\times10^{-7}$	q_m	K_L
NZ-BR_{46}	0.974	2.594	0.0130	17.770
NaZ-BR_{46}	0.982	3.138	0.0156	36
HZ-BR_{46}	0.954	0.16	0.0230	25.50
NZ-BY13	0.982	0.108	0.0085	41.301
NaZ-BY_{13}	0.991	0.120	0.0131	34.121
HZ-BY13	0.988	0.374	0.0201	49.885

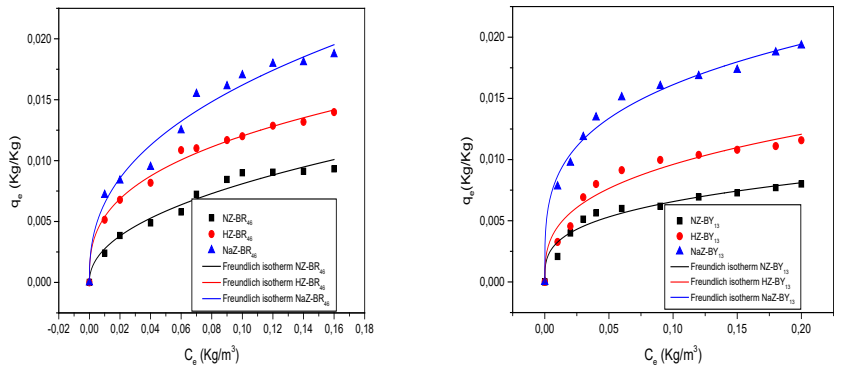

Figure 11 – Non-linear Freundlish adsorption isotherms for BR_{46} and BY_{13}

Table 5 – Freundlish model constants of BR_{46} and BY_{13} removal on NZ, NaZ, and HZ

	R^2	$\chi^2 \times 10^{-7}$	K_f	n
		BR_{46}		
NZ-BR_{46}	0.978	3.23	0.023	2.138
HZ-BR_{46}	0.999	1.493	0.026	2.868
NaZ-BR_{46}	0.978	9.187	0.040	2.533
		BY_{13}		
NZ-BY_{13}	0.978	2.671	0.013	3.282
HZ-BY_{13}	0.987	6.519	0.020	3.033
NaZ-BY_{13}	0.984	4.068	0.03	3.075

By analyzing the correlation coefficient (R^2) presented in Tables 4 and 5, it can be observed that the adsorption of dyes onto natural and activated zeolites follows both the Freundlich and the Langmuir isotherm model. These results imply that both monolayer and multilayer adsorption processes may occur simultaneously, and the zeolites surface exhibit both homogeneous and heterogeneous characteristics (Tian et al, 2016). Moreover, the values of n (Table 5) are greater than 1, suggesting a favorable adsorption process. These findings are consistent with the results reported by **(**Karadag et al, 2007**).**

Effect of pH

The influence of pH on dye adsorption was investigated by variying the initial solution pH (pH_0) from 3 to 10 at 25 °C298 K. Adjustments were made using 100 mol/m^3 HCl or 100 mol/m^3 NaOH, while ensuring that all other experimental conditions remained constant.

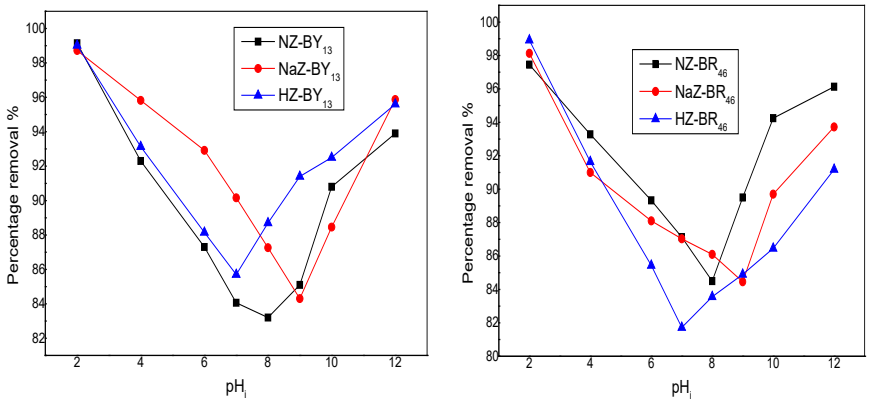

Figure 12 – Effect of pH of the dye solution on the removal of dyes by NZ,HZ, and NaZ

As shown in Figure 12, the dye removal percentage initially decreased with pH up to a certain level for the three zeolites before increasing. The lowest removal percentages were observed at pH 8 for NZ, pH 9 for NaZ, and pH 7 for HZ. This trend can be attributed to the variations in the surface charge of each zeolite and the degree of dye ionization. In the acid medium, the presence of H^+ creates competition with the dyes. At neutral pH, protons and hydroxides are in equilibrium, while at higher pH, OH^- dominates. The observed fluctuations in the removal efficiency can be effectively explained by the point of zero charge (PHZ).

Comparing the pH_i and the PHZ values of NZ, NaZ, and HZ, it was found that at the pH levels below the PHZ, the zeolite surfaces became positively charged, favoring anion adsorption over cations. However, at the pH levels above the PHZ, negative charges on the zeolites dominated, leading to a preference for cation adsorption.

Thermodynamics of adsorption

Table 6 presents the thermodynamic parameters ΔG, ΔH, and ΔS for the adsorption of BR_{46} and BY_{13} on NZ, HZ, and NaZ. The negative values of ΔG at all temperatures indicate that the adsorption process is both spontaneous and thermodynamically favorable. Furthermorer, as the temperature increases, ΔG values decrease, suggesting that higher temperatures enhance the favorability of adsorption. The positive values of ΔH confirm that the adsorption process is endothermic. Additionally, the positive values of ΔS indicate an increase in randomness at the solid-liquid interface during adsorption, for both natural and activated zeolites. These findings are consistent with the previous studies conducted by Karadag et al. **(**Karadag et al, 2007**).**

Table 6 – Thermodynamic parameters of BR_{46} and BY_{13} adsorption on NZ, HZ, and NaZ

	BY_{13}					**BR_{46}**				
	ΔG° (kJ/mol K)			ΔH° (kJ/mol)	ΔS° (J/mol)	ΔG°			ΔH° kJ/mol K	ΔS° J/mol K
	298K	**313K**	**323K**			**298K**	**313K**	**323K**		
NZ	-6.055	-24.55	-33.80	264.97 0.925		-13.87	-26.77	-35.37	242.41 0.86	
NaZ	-8.29	-21.04	-29.54	245.01	0.85	-16.48	-28.53	-36.56	222.81	0.803
HZ	-11.36	-25.83	-35.48	276.21	0.965	-14.85	-27.17	-35.38	229.8	0.821

Conclusion

This study investigated the effect of modifying natural mordenite zeolite with low concentrations of acid and alkaline solutions on the removal of cationic textile dyes from aqueous solutions, comparing their adsorption affinities. XRF and SEM-EDX analyses revealed that the HCl treatment removed Al, while the NaOH treatment removed Si from the zeolite surface, reducing their external framework content while preserving the primary structure. FTIR spectroscopy indicated shifts, disappearance of bands, and decreases in certain peaks for NaZ and HZ, attributed to cation replacement by hydronium inons or the removal of aluminium and silicon. These structural changes also influenced the PHZ of both natural and modified zeolites. The results showed that NaZ exhibited the highest removal efficiency compared to NZ and HZ for cationic dyes in aqueous solutions. Equilibrium was reached gradually, stabilizing due to the high number of active sites on the zeolite surface. The adsorption of BR_{46} and BY_{13} on NZ, NaZ, and HZ was described by both the Langmuir and the Freundlich models, while the pseudo-second-order model accurately represented the adsorption process. The adsorption onto zeolites is governed by a combination of film diffusion and intraparticle diffusion, with zeolite modification significantly influencing diffusion kinetics. Thermodynamic analysis indicated that dye adsorption was spontaneous, random and endothermic.

References:

Aarden, F.B. 2001. *Adsorption onto heterogeneous porous materials: equilibria and kinetics*, Technische Universiteit Eindhoven. ISBN: 90-386-2822-6

Amin, G., Konstantinovic, S., Jordanov, I. & Djordjevic, D. 2023. Adsorption study of textile dye Basic Red 46 on clinoptilolite. *Iran J Chem Chem Eng.,* 5428. Available at: http://doi.org/10.30492/ijcce.2023.557165.5428

Aravindhan, S., Kumar, G.B., Saravanan, M. & Arumugam, A. 2023. Delonix regia biomass as an eco-friendly biosorbent for effective Alizarin Red S textile dye removal: Characterization, kinetics, and isotherm studies. *Bioresource Technology Reports*, 101721. Available at: https://doi.org/10.1016/j.biteb.2023.101721

Ates, A. & Akgül, G. 2016. Modification of natural zeolite with NaOH for removal of manganese in drinking water. *Powder technology,* 287, 285-291. Available at: http://doi.org/10.1016/j.powtec.2015.10.021

Ebsa, D.G. 2023. Defluoridation of drinking water by modified natural zeolite with Cationic surfactant, in the case of Ziway town, Ethiopia. *Cleaner Engineering and Technology,* 12, 100596. Available at: http://doi.org/10.1016/j.clet.2023.100596

Garcia-Basabe, Y., Rodriguez-Iznaga, I., De Menorval, L.-C., Llewellyn, P., Maurin, G., Lewis, D.W., Binions, R., Autie, M. & Ruiz-Salvador, A.R. 2010. Step-wise dealumination of natural clinoptilolite: Structural and physicochemical characterization. *Microporous and Mesoporous Materials,* 135**,** 187-196. Available at: http://doi.org/10.1016/j.micromeso.2010.07.008

Ho, Y. & Mckay, G. 1998. A comparison of chemisorption kinetic models applied to pollutant removal on various sorbents. *Process safety and environmental protection,* 76**,** 332-340. Available at: http://doi.org/10.1205/095758298529696

Ighnih, H., Haounati, R., Ouachtak, H., Regti, A., El Ibrahimi, B., Hafid, N., Jada, A., Taha, M.L. & Addi, A.A. 2023. Efficient Removal of Hazardous Dye from Aqueous Solutions Using Magnetic Kaolinite Nanocomposite: Experimental and Monte Carlo Simulation Studies. *Inorganic Chemistry Communications***,** 110886. Available at: http://doi.org/10.1016/j.inoche.2023.110886

Imessaoudene, A., Mechraoui, O., Aberkane, B., Benabbas, A., Manseri, A., Moussaoui, Y., Bollinger, J.-C., Amrane, A., Zoukel, A. & Mouni, L. 2024. Synthesis of a TiO2/zeolite composite: Evaluation of adsorption-photodegradation synergy for the removal of Malachite Green. *Nano-Structures & Nano-Objects,* 38**,** 101191. Available at: http://doi.org/10.1016/j.nanoso.2024.101191

Karadag, D., Akgul, E., Tok, S., Erturk, F., Kaya, M.A. & Turan, M. 2007. Basic and reactive dye removal using natural and modified zeolites. *Journal of Chemical & Engineering Data,* 52**,** 2436-2441. Available at: http://doi.org/10.1021/je7003726

Kumar, N., Pandey, A. & Sharma, Y.C. 2023. A review on sustainable mesoporous activated carbon as adsorbent for efficient removal of hazardous dyes from industrial wastewater. *Journal of Water Process Engineering,* 54**,** 104054. Available at: http://doi.org/10.1016/j.jwpe.2023.104054

Lagergren, S. 1898. *About the theory of so-called adsorption of solution substances* [Online]. Available: https://sid.ir/paper/563615/en [Accessed].

Lellis, B., Fávaro-Polonio, C.Z., Pamphile, J.A. & Polonio, J.C. 2019. Effects of textile dyes on health and the environment and bioremediation potential of living organisms. *Biotechnology Research and Innovation,* 3**,** 275-290. Available at: http://doi.org/10.1016/j.biori.2019.09.001

Li, H., Liu, S., Zhao, J. & Feng, N. 2016. Removal of reactive dyes from wastewater assisted with kaolin clay by magnesium hydroxide coagulation process. *Colloids and Surfaces A: Physicochemical and Engineering Aspects,* 494**,** 222-227. Available at: http://doi.org/10.1016/j.colsurfa.2016.01.048

Lycourghiotis, S., Makarouni, D., Kordouli, E., Bourikas, K., Kordulis, C. & Dourtoglou, V. 2018. Activation of natural mordenite by various acids: Characterization and evaluation in the transformation of limonene into p-cymene. *Molecular Catalysis,* 450**,** 95-103. Available at: http://doi.org/10.1016/j.mcat.2018.03.013

Mamo, W., Awoke, Y., Chebude, Y. & Diaz, I. 2015. Mild modification method for the generation of mesoporosity in synthetic and natural mordenite. *Bulletin of*

the Chemical Society of Ethiopia, 29**,** 95-103. Available at: http://doi.org/10.4314/bcse.v29i1.8

Mehdi, B., Belkacemi, H., Brahmi-Ingrachen, D., Braham, L.A. & Muhr, L. 2022. Study of nickel adsorption on NaCl-modified natural zeolite using response surface methodology and kinetics modeling. *Groundwater for Sustainable Development,* 17**,** 100757. Available at: http://doi.org/10.1016/j.gsd.2022.100757

Nakamoto, K., Ohshiro, M. & Kobayashi, T. 2017. Mordenite zeolite—Polyethersulfone composite fibers developed for decontamination of heavy metal ions. *Journal of Environmental Chemical Engineering,* 5**,** 513-525. Available at: http://doi.org/10.1016/j.jece.2016.12.031

Pastukhov, A.V., Ilyin, M.M. & Chkanikov, N.D. 2023. Acid-activated natural zeolite and montmorillonite as adsorbents decomposing metsulfuron-methyl herbicide. *Inorganic Chemistry Communications,* 158**,** 111615. Available at: http://doi.org/10.1016/j.inoche.2023.111615

Reeve, P.J. & Fallowfield, H.J. 2018. Natural and surfactant modified zeolites: A review of their applications for water remediation with a focus on surfactant desorption and toxicity towards microorganisms. *Journal of environmental management,* 205**,** 253-261. Available at: http://doi.org/10.1016/j.jenvman.2017.09.077

Selim, K., Youssef, M., Abd El-Rahiem, F. & Hassan, M. 2014. Dye removal using some surface modified silicate minerals. *International Journal of Mining Science and Technology,* 24**,** 183-189. Available at: http://doi.org/10.1016/j.ijmst.2014.01.007

Senguttuvan, S., Janaki, V., Senthilkumar, P. & Kamala-Kannan, S. 2022. Polypyrrole/zeolite composite–A nanoadsorbent for reactive dyes removal from synthetic solution. *Chemosphere,* 287**,** 132164. Available at: http://doi.org/10.1016/j.chemosphere.2021.132164

Tian, J., Guan, J., Gao, H., Wen, Y. & Ren, Z. 2016. The adsorption and mass-transfer process of cationic red X-GRL dye on natural zeolite. *Water Science and Technology,* 73**,** 2119-2131. Available at: http://doi.org/10.2166/wst.2016.055

Visa, M. 2016. Synthesis and characterization of new zeolite materials obtained from fly ash for heavy metals removal in advanced wastewater treatment. *Powder Technology,* 294**,** 338-347. Available at: http://doi.org/10.1016/j.powtec.2016.02.019

Wang, C., Wang, L., Du, F., Yu, Q. & Liang, X. 2023. A two-step organic modification strategy for improving surface hydrophobicity of zeolites. *Advanced Powder Technology,* 34**,** 104228. Available at: http://doi.org/10.1016/j.apt.2023.104228

Weber Jr, W.J. & Morris, J.C. 1964. Equilibria and capacities for adsorption on carbon. *Journal of the Sanitary Engineering Division,* 90**,** 79-108. Available at: http://doi.org/10.1061/JSEDAI.0000496

Eliminación de colorantes textiles básicos del agua mediante zeolita argelina natural y modificada: estudios cinéticos, termodinámicos y de equilibrio

Nassima Belgaid[a], **autor de correspondencia,** *Mohamed Redha* Menani[b], *Kamel Eddine* Bouhidel[b]

[a] Universidad de Batna 2, Laboratorio de Movilización y Gestión de Recursos Hídricos (MGRE), Instituto de Ciencias de la Tierra y del Universo, 53, carretera de Constantina, Fesdis, Batna 05078, República de Argelia.
[b] Universidad de Batna 1, Laboratorio de Química y Química Ambiental (LCCE), Departamento de Química, Facultad de Ciencias de la Materia, Carretera de Biskra, Batna 05000, República de Argelia

CAMPO: Tecnologías químicas
CATEGORÍA (TIPO) DEL ARTÍCULO: original de la investigación científica,

Resumen:

Introducción/objetivo: La zeolita natural argelina (denominada NZ) se modificó mediante ácido clorhídrico (HZ) y solución de hidróxido de sodio (Na2). Este estudio investigó el efecto de las modificaciones ácidas y alcalinas en la adsorción de dos colorantes textiles catiónicos (BR46 y BY13) en soluciones acuosas.

Métodos: : El análisis XRF confirmó que el SiO_2 es el mineral predominante en las tres zeolitas. Los resultados de XRD revelaron que la NZ está compuesta principalmente de mordenita, con chabasita y un contenido menor de cuarzo. El análisis MEB-EDX mostró ligeras variaciones en el contenido de Si y Al para HZ y NaZ, sin alterar significativamente la estructura de la zeolita. Se examinaron los efectos de la concentración inicial del tinte, el tiempo de contacto y el pH en un sistema por lotes.

Resultados: La adsorción en NZ, NaZ y HZ aumentó con tiempos de contacto más largos, mayores concentraciones iniciales de colorante y temperaturas elevadas. El equilibrio se alcanzó rápidamente, lo cual se describe mejor mediante el modelo cinético de pseudo-segundo orden. Los modelos de isotermas de Langmuir y Freundlich son compatibles con los datos de adsorción.

Conclusión: La mayor eficiencia de eliminación de colorante se observó para NaZ, con un 97,62 % para BR_{46} y un 98,97 % para BY_{13}. Las tasas de eliminación más bajas se obtuvieron a pH = 8 para HZ y pH = 10 para NZ y NaZ. La adsorción fue espontánea y endotérmica.

Palabras claves: zeolita, modificación, ácido, alcalino, adsorción, colorantes catiónicos

Belgaid, N et al, Removal of basic textile dyes from water by natural and modified Algerian zeolite: kinetic, thermodynamic and equilibrium studies, pp1017-1044.

Удаление основных текстильных красителей из воды природным и модифицированным алжирским цеолитом: исследования кинетического, термодинамического и равновесного состояний

Нассима Белгайд[а], **корреспондент,** *Мохамед Редха* Менани[б], *Камель Эддин* Бухидель[б]

[а] Университет Батны, 2, лаборатория мобилизации и управлением водными ресурсами (MGR), Научный институт о Земле и космосе, дорога Константина 53, Фесдис, Батна 05078, Алжирская Народная Демократическая Республика Алжир.

[б] Университет Батны 1, лаборатория химии и охраны окружающей среды химический институт, факультет материаловедения, дорога Бискра, Батна, 05000, Алжирская Народная Демократическая Республика

РУБРИКА ГРНТИ: 61.13.21 Химические процессы
ВИД СТАТЬИ: оригинальная научная статья

Резюме:

Введение/цель: Алжирский природный цеолит (обозначаемый как NZ) был модифицирован с помощью соляной кислоты (HZ) и раствора гидроксида натрия (NaZ). В данном исследовании изучено влияние кислотных и щелочных модификаций на адсорбцию двух катионных текстильных красителей (BR46 и BY13) из водных растворов.

Методы: Рентгенофазовый анализ подтвердил, что SiO2 является преобладающим минералом во всех трех цеолитах. Результаты рентгенофазового анализа показали, что NZ в основном состоит из морденита с небольшим содержанием шабазита и кварца. Анализ MEB-EDX показал незначительные изменения в содержании Si и Al в HZ и NaZ без существенного изменения структуры цеолита. Влияние начальной концентрации красителя, времени контакта и pH было исследовано по сериям.

Результаты: Адсорбция NZ, NaZ и HZ увеличивалась при более продолжительном времени контакта, увеличении начальной концентрации красителя и повышении температуры. Баланс был быстро установлен, что лучше всего описывается с помощью кинетической модели псевдо-второго порядка. Для получения данных об адсорбции подходят как модели изотерм Ленгмюра, так и Фрейндлиха.

Выводы: Самая высокая эффективность удаления красителя наблюдалась у NaZ − 97,62% для BR_{46} и 98,97% для BY_{13}. Наименьшая скорость удаления наблюдалась при pH = 8 у HZ и pH=10 у NZ и NaZ. Адсорбция была спонтанной и эндотермической.

Ключевые слова: цеолит, модификация, кислота, щелочь, адсорбция, катионные красители.

Уклањање основних текстилних боја из воде помоћу природног и модификованог алжирског зеолита: студије из кинетике, термодинамике и равнотежних стања

Насима Белгаид[а], **аутор за преписку,** *Мохамед Редха* Менани[б], *Камел Един* Бухидел [б]

[а] Универзитет у Батни 2, Лабораторија за мобилизацију и управљање водним ресурсима, Институт за земљане науке и универзум, Фесдис, Батна, Република Алжир

[б] Универзитет у Батни 1, Лабораторија хемије и еколошке хемије, Одсек за хемију, Факултет за науку о материјалу, Батна, Република Алжир

ОБЛАСТ: хемијска технологија
КАТЕГОРИЈА (ТИП) ЧЛАНКА: оригинални научни рад

Сажетак:

Увод/циљ: Природни зеолит (NZ) из Алжира модификован је помоћу хлороводоничне киселине (HZ) и раствора натријум-хидроксида (NaZ). Ова студија испитује утицај модификација киселином и базом на адсорпцију две катјонске боје за текстил (BR_{46} и BY_{13}) из водених раствора

Методе: Анализа XRF је потврдила да минерал SiO2 преовлађује у сва три зеолита. Резултати анализе XRD указују да се NZ превасходно састоји од морденита, уз хабазит и мањи садржај кварца. Анализа MEB-EDX је показала мање варијације у садржају Si и Al код HZ и NaZ, без значајне промене у структури зеолита. Утицаји почетне концентрације боје, времена контакта и pH вредности испитани су по серијама.

Резултати: Адсорпција NZ, NaZ и HZ повећала се са дужим временима контакта, вишим почетним концентрацијама боје и повишеним температурама. Равнотежа је брзо била постигнута, што је најбоље описано кинетичким моделом псеудодругог реда. Изотермни модели и по Лангмиру и по Фројндлиху одговарају адсорпционим подацима.

Закључак: Најефикасније уклањање боје уочено је код NaZ (97,62% за BR_{46} и 98,97% за BY_{13}) . Најниже брзине уклањања биле су за pH= 8 код HZ и за pH=10 код NZ и NaZ. Адсорпција је била спонтана и ендотермна.

Кључне речи: зеолит, модификација, киселост, алкалност, адсорпција, катјонске боје

Paper received on: 18.01.2025.
Manuscript corrections submitted on:12.02.2025
Paper accepted for publishing on: 25.02.2025.